

Supplementary Information

Stereoselective coronas regulate the fate of chiral gold nanoparticles *in vivo*

Didar Baimanov,^{1,2,#} Liming Wang,^{1,#} Ke Liu,^{1,3,#} Mengmeng Pan,² Rui Cai,¹ Hao Yuan,¹
Wanxia Huang,⁴ Qingxi Yuan,⁴ Yunlong Zhou,^{2,*} Chunying Chen^{1,5,6,*} and Yuliang
Zhao^{1,5,6,*}

¹ CAS Key Laboratory for Biomedical Effects of Nanomaterials and Nanosafety, CAS Center for Excellence in Nanoscience, CAS-HKU Joint Laboratory of Metallomics on Health and Environment, National Center for Nanoscience and Technology of China and Institute of High Energy Physics, Chinese Academy of Sciences, Beijing 100190, P. R. China

² Engineering Research Center of Clinical Functional Materials and Diagnosis & Treatment Devices of Zhejiang Province, Wenzhou Institute, University of Chinese Academy of Sciences, Wenzhou 325000, P. R. China

³ College of Materials and Chemistry & Chemical Engineering, Chengdu University of Technology, Sichuan province, Chengdu 610059, P. R. China

⁴ Beijing Synchrotron Radiation Facility, Institute of High Energy Physics, Chinese Academy of Sciences, Beijing 100049, P. R. China

⁵ GBA Research Innovation Institute for Nanotechnology, Guangzhou 510700, Guangdong, P. R. China

⁶ Research Unit of Nanoscience and Technology, Chinese Academy of Medical Sciences, Beijing 100730, P. R. China

These authors contributed equally

* Correspondence and requests for materials should be addressed to Y. Zhao (zhaoyl@nanoctr.cn), C.C. (chenchy@nanoctr.cn) or Y.Zhou (zhouyl@ucas.ac.cn)

Methods

Materials. Tetrachloroauric (III) trihydrate ($\text{HAuCl}_4 \cdot 3\text{H}_2\text{O}$, 99.9%), and sodium borohydride (NaBH_4 , 99%) were purchased from Sigma-Aldrich. L-Ser-L-Cys-L-Ser and D-Ser-D-Cys-D-Ser (tripeptide, 98%) were purchased from KE Biochem Co., Ltd. β -mercaptoethanol and phorbol 12-myristate 13-acetate (PMA) were purchased from Macklin Biochemical Co., Ltd. Penicillin–streptomycin (PS), 2-[4-(2-hydroxyethyl)piperazin-1-yl]ethanesulfonic acid (HEPES), phosphate buffer saline (PBS), and RPMI 1640 cell culture medium were purchased from Wisent Corporation. Fetal bovine serum (FBS) was purchased from Biological Industries (BI). Human apolipoprotein CIII (ApoC3), ApoA1, ApoE, clusterin, fibrinogen, fibronectin, complement C3, C1q, and C4 proteins were purchased from Beijing Chengzhi Kewei Biotechnology Co., Ltd. Immunoglobulin G was purchased from Sigma-Aldrich. An anti-LDL receptor antibody was purchased from Abcam. Human TNF- α , IL-6, and IL-1 β ELISA kits were purchased from Thermo Fisher. The bicinchoninic acid assay (BCA assay) was purchased from Thermo Fisher Scientific. The TRIZOL reagent was purchased from Life Technology. Moloney murine leukemia virus reverse transcriptase (M-MLV) and Master Mix were purchased from Promega. SYBR Green was purchased from Invitrogen. The primers were purchased from synthesized by Sangon Biotech. The blood plasma collection tubes for animal experiments were purchased from BD Vacutainer™. Mouse Apolipoprotein E (ApoE), Apo-A1, ApoC3, clusterin ELISA kits were purchased from Jiangsu Meimian industrial Co., Ltd. C57BL/6J mice were purchased from the SPF (Beijing) Biotechnology Co., Ltd. Ultrapure water was obtained from a Millipore filter system.

Synthesis of chiral gold nanoparticles. Typically, an aqueous solution of $\text{HAuCl}_4 \times 3\text{H}_2\text{O}$ (175 μL , 50 mM) was added to a 10mL fresh chiral tripeptide aqueous solution (0.025 mmol), the yellow solution gradually turned colorless or light yellow. After continuous stirring for half an hour, 2 mL NaBH_4 aqueous solution (0.20 mmol) was added slowly with rapid stirring to fully reduce the gold ions, and then the solution was stirred for another 2 h until the solution became a dark red color. The resultant product was collected by cut-off filtration at 8,000 \times rpm for 10 min and then washed three times with deionized water to remove free molecules. Finally, the chiral gold nanoparticles were dispersed in an aqueous solution and stored at 4 $^\circ\text{C}$ until used.

Characterization of chiral gold nanoparticles. Circular dichroism (CD) spectra were obtained with a J-1500 CD spectrometer (Jasco, Japan) under high-purity nitrogen at 25 $^\circ\text{C}$ for all measurements, using a scanning range of 195-300 nm. High-resolution TEM measurements were obtained with a Tecnai G2 20 S-TWIN with an accelerating voltage of 200 kV. Ultraviolet-visible (UV-Vis) spectra were obtained with a UV-Vis spectrophotometer. The hydrodynamic diameter and surface charge of chiral gold nanoparticles were obtained with a Zetasizer Nano ZS dynamic light scattering instrument (Malvern Instruments, UK). The concentration of Au in the gold nanoparticles was quantified with a Thermo Elemental X7 ICP-MS¹.

Preparing human blood serum. Blood was collected from healthy volunteers, which were obtained from IHEP Institute Clinic, with the approval of the institute's ethics committee, and complied with all relevant ethical regulations. Further, blood was allowed to clot at room temperature for 30 min, and centrifuged at 1,100-1,300 \times g for 20 minutes to pellet the red and white blood cells. The supernatant (serum) was collected and purified

from insoluble debris and aggregated proteins, as well as remaining red and white blood cells by additional centrifugation at $10,000 \times g$ for 5 min at 4°C . Obtained serum was transferred in 1.5 ml tubes, aliquoted by 0.5 mL serum per tube, labeled, and stored at -80°C until further use.

Obtaining stereoselective coronal fingerprints. All experiments were conducted with three biological replicates to ensure the reproducibility of the obtained proteomics results. Prior to the experiments, the human serum was centrifuged at $10,000 \times g$ for 5 min at 4°C to remove any insoluble debris and aggregated proteins. To ensure the condition of the serum proteins, each tube with aliquoted serum was used upon melting without repeated freeze. Chiral gold nanoparticles (1 mg/mL, $n=3$, 100 μL) were introduced to 10% human serum and incubated at 37°C for 1 h under continuous stirring to allow the formation of a long-lived hard protein coronas, after which centrifugation was performed to isolate corona complexes ($18,800 \times g$, 15 min). The pellet was washed in ice-cold PBS three times. Finally, coronal proteins were eluted by adding 5% SDS buffer (100 μL) to the pellet and were heated at 95°C for 15 min to denature and strip proteins from chiral gold nanoparticles. The total protein concentrations were determined using the BCA assay kit according to the manufacturer's instructions. Coronated chiral gold nanoparticles were imaged with a HITACHI H-7000FA with an accelerating voltage of 100 kV after negative staining.

LC-MS/MS. Eluted coronal proteins were digested, and obtained products were separated by using a Thermo Ultimate 3000 nano-UPLC system directly interfaced with a Thermo Fusion LUMOS mass spectrometer. The Fusion LUMOS mass spectrometer was operated in data-dependent acquisition mode using Xcalibur 4.1.50 software, and there was a single

full-scan mass spectrum in the Orbitrap (350–1800 m/z, 60,000 resolution), followed by 20 data-dependent MS/MS scans. MS/MS spectra from each LC-MS/MS run were searched against the human database using the software Proteome Discoverer (Thermo Scientific, version 2.4). The minimum number of peptides with a length of 6–144 amino acids for protein identification was set as one. Peptide FDR was set as 0.01 and protein FDR was set as 0.05. Identified corona proteins on chiral NPs were manually assigned *via* searching against the human protein database in the UniProt database (<https://www.uniprot.org>). The relative abundance for each protein was calculated based on label-free quantification intensities relative to the total sum of protein intensities for each sample. To determine the enrichment of the coronal proteins, the enrichment factor was calculated based on relative abundance (mean of triplicate biological samples) of coronal protein over serum protein.

Microscale thermophoresis assay (MST). The affinity of the serum protein with chiral gold nanoparticles was calculated using Monolith NT. 115 (NanoTemper Technologies GmbH). Protein concentration was adjusted to 2–20 μM and was labeled with RED-NHS fluorescent dye *via* incubation for 30 min at room temperature in the dark, followed by further column purification. Chiral gold nanoparticles at varying concentrations (from 0.001 nM to 40 nM) were introduced to 20 nM of labeled proteins at room temperature for 5 min. The sample was loaded into NanoTemper hydrophilic treated capillaries and was measured at 24 °C using 20% LED power and 80% MST power. All experiments were repeated three times. Data analyses were carried out using NanoTemper analysis software. The molar concentration of chiral gold nanoparticles was measured and calculated by using Nanosight (Malvern).

STRING. The top twenty-five most abundant proteins and possible cell receptors were input into the STRING² webserver, to predict protein- protein associations experimental interactions scores were determined. We used a STRING threshold of 0.80 to filter our list of predicted interactions, the complete list of predicted interactions with scores was listed in Table S3, ESI.

Cell culture. THP-1 cells were purchased from Procell Life Science and Technology Co. Ltd. and were cultured in RPMI-1640 supplemented with heat-inactivated 10% FBS, 1% penicillin–streptomycin, 1% HEPES, and 2 μ L of β -mercaptoethanol. THP-1 cells were differentiated (10 ng/mL PMA) onto six-well plates at a density of 1×10^6 cells/well for 48 h. The differentiated macrophages were inspected by using an optical microscope, and after the removal of PMA³ by a triplicated wash with PBS, we incubated cells in a complete cell medium for an additional 24 h. Next, chiral gold nanoparticles (20 μ g/mL) supplied with 10% human serum were introduced to differentiated macrophages. The supernatant was collected, and the levels of IL-6, IL-1 β , and TNF- α were measured using ELISA kits according to the manufacturer’s protocol. The three independent experiments were performed, and all results were expressed in pg/mL. Although fetal bovine serum was used for cell culturing, we chose human serum as culturing condition, which can roughly correlate with the *in vitro* obtained protein corona.

To observe the cellular uptake by TEM, treated macrophages were collected, kept at 4 $^{\circ}$ C, and immobilized with 2.5% glutaraldehyde for 4 h. The dehydrated cells were sectioned \sim 60 nm slices and transferred to Formvar-coated copper grids. After staining with uranyl acetate and Reynolds lead citrate, the cell sections were observed using TEM at 120 kV.

RT-qPCR. THP-1 cells were differentiated onto 6-well plates at a density of 1×10^6 cells/well for 48 h. RT-qPCR experiments were done to determine the level of mRNA expression. The TRIZOL reagent method was used to isolate RNA from cells. Each sample was prepared for real-time quantitative PCR in a final reaction volume of 20 μ L by adding Master Mix and SYBR Green. The amplification cycle was performed by Realplex4 (Eppendorf).

The primer sequences were shown below:

Primers	Forward	Reverse
GAPDH	GGGAGCCAAAAGGGTCATCA	AAAGTGGTCGTTGAGGGCAA
IL-1 β	CCAGCTACGAATCTCCGACC	GGGAACTGGGCAGACTCAAA
TNF- α	ACAATAGGCTGTTCCCAT	AAACTTTATTTCTCGCCACT
IL-6	GGATTCAATGAGGAGACTTGCC	TGGCATTGTGGTTGGGTCA
LDLR	CCATCTCAAGCATCGATGTCAAC	TCTGATAGACGGGGTTGTCAAAG
ITGAM	CAGCCTTGTTTCCCTTTGAGAAG	GGTTGCTGACCTGATATTGATGC
CD36	ATGTGCAAAATCCACAGGAAGTG	TCAACAAAAGGTGGAAATGAGGC
FCGR2A	GCTTCAACCATTGACAGTTTTGC	GTTTCCTGTGCAGTGGTAATCAC
TLR2	CTGTCCAACAACAGGATCACCTA	TCAGTATCTCGCAGTTCCAAACA
MSR1	TGGGAACATTCTCAGACCTTGAG	CCCCCATTGCCGAATTTTACATT

Cellular uptake of chiral gold nanoparticles. THP-1 cells were differentiated onto 6-well plates at a density of 1×10^6 cells/well for 48 h. It should be noted that cells were cultured and differentiated in a cell culture medium supplied with 10% FBS. However, a complete cell culture medium containing 10% human serum was used for stereoselective cellular uptake experiments. To study the effect of different proteins on cellular uptake, serum-free RPMI 1640 medium supplemented with a protein solution (10 μ g/mL). To study the effect of LDLR antibody on cellular uptake, LDLR receptors of differentiated macrophages were

blocked with LDLR antibody solution (1 $\mu\text{g}/\text{mL}$) for 1 h at 37 $^{\circ}\text{C}$. Then the medium was replaced by fresh medium with chiral gold nanoparticles supplied with serum protein for 24 h at 37 $^{\circ}\text{C}$. In detail, apolipoproteins mediated the stereoselective recognition of chiral gold nanoparticle by macrophages. Therefore, we attempt to determine the role of LDLR on stereoselective uptake, by blocking the receptors with antibody followed by incubation of chiral gold nanoparticles in protein-supplied medium (Figure 4e and g). Furthermore, due to the significant stereoselectivity of complement C3 protein (LC-MS/MS and MST), we hypothesized that immunoglobulin G might mediate the complement C3 activation, resulting in stereoselective recognition by macrophages (Figure 4i). Cellular uptake of chiral gold nanoparticles was further evaluated using ICP-MS, followed by our previously reported protocols.

***In vivo* biodistribution of chiral gold nanoparticles.** Pathogen-free C57BL/6 mice (female, 6–8 weeks old) were used in this study. All the animals were maintained on a standard diet and water ad libitum at 22 ± 2 $^{\circ}\text{C}$ and 50–60% relative humidity on a 12 h light/12 h dark cycle. All protocols were approved by the Institutional Animal Care and Use Committee of the National Center for Nanoscience and Technology and performed under the ethical guidelines for the use and care of animals. L-Au NPs or D-Au NPs at the dose of 5 mg/kg (n=5) were intravenously injected into the tail vein of female C57BL/6 mice. Blood and organs (liver, spleen, lung, kidney, and heart) were harvested at 3 – 72 hours post-injection and stored at -80 $^{\circ}\text{C}$ before ICP-MS measurements¹. Further, *in vivo* biodistribution of chiral gold nanoparticles was evaluated based on Au concentration using ICP-MS. Mouse blood was collected and allowed to clot at room temperature for 30 min, and mouse serum was collected by centrifugation at 1,100-1,300 \times g for 20 minutes.

Collected mouse serum was additionally purified from cell debris and protein aggregates by centrifugation and stored at $-80\text{ }^{\circ}\text{C}$ before ELISA experiments. *Ex vivo* serum lipoprotein level was quantified using an ELISA kit following the manufacturer's protocol. The possible influence of the chiral gold nanoparticles remaining in the sera collected at different time points of post-injection on the detected lipoproteins level was not addressed in this study.

SR micro-CT. The livers of control and chiral gold nanoparticles-treated mice were collected at a 24-hour post-injection time point. In order to maintain their morphology and prevent any changes during imaging, the liver samples were preserved in a 4% formaldehyde solution. One liver lobe was dissected and loaded into the synchrotron radiation micro-CT instrument for imaging after the samples had been prepared. The scanning parameters involved a 12 keV beam energy with a 1.5 s exposure using the 2X objective and Hamamatsu C15550-20UP detector for scan. The SR micro-CT imaging was conducted at Beamline 4W1A of the Beijing Synchrotron Radiation Facility (BSRF), China. The results obtained were processed and visualized using Avizo v. 2019.1 software.

Statistical analysis. All the data were presented with the mean \pm standard deviation (s.d.). For the statistical significance of differences, ANOVA analysis was performed using GraphPad Prism (version 8.2.1, USA). If significance was determined, a two-way ANOVA posthoc multiple comparison analysis was conducted with the Tukey test. A two-sided student's t-test was used to assess the difference between the two groups for cellular uptake experiments. **** $p < 0.0001$, *** $p < 0.001$, ** $p < 0.01$, * $p < 0.05$.

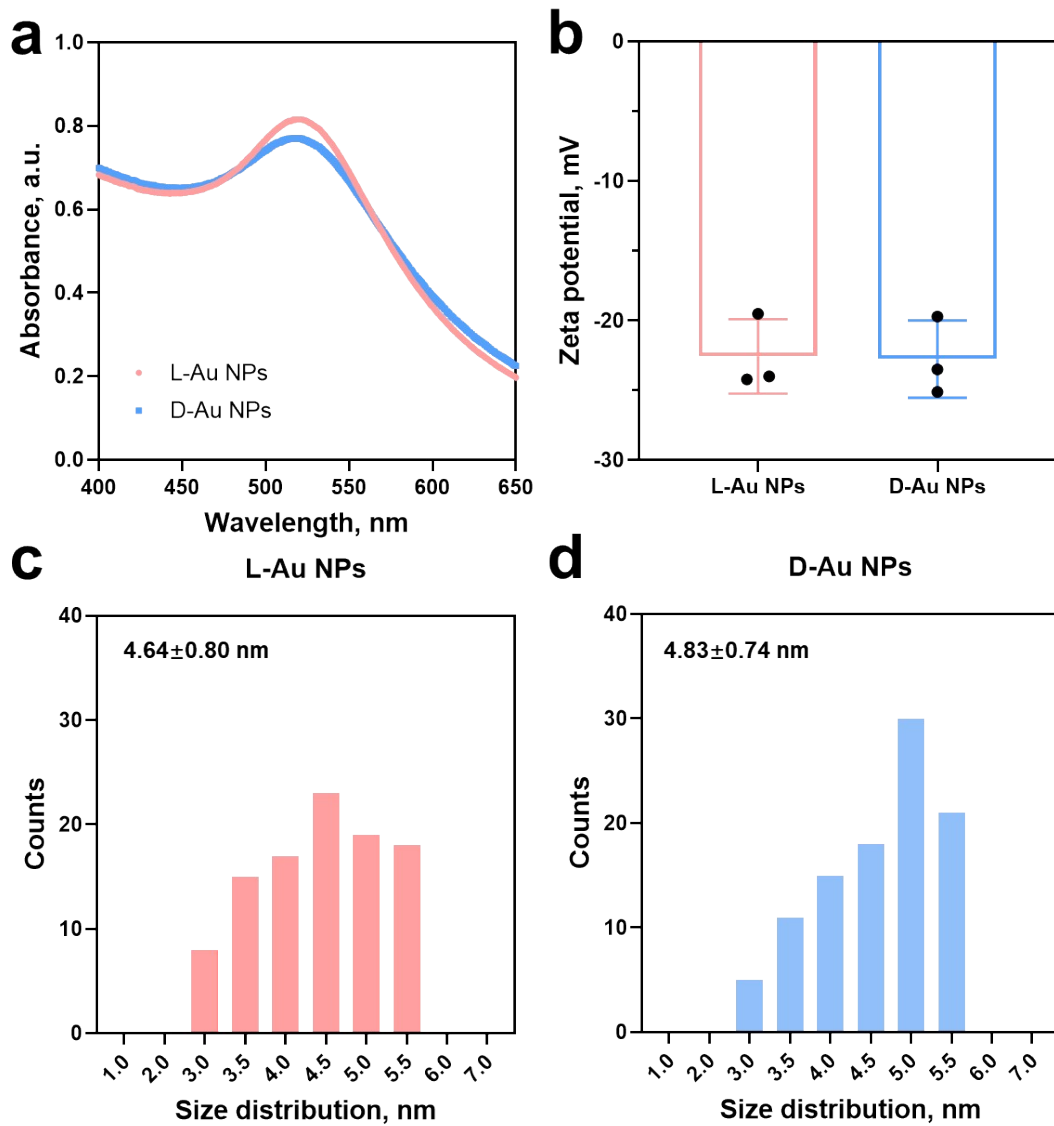


Figure S1. UV-vis spectroscopy (a) and Zeta-potential (b) of chiral gold nanoparticle. Chiral gold nanoparticles are stabilized by tripeptides: L-Au NPs (red) and D-Au NPs (blue). Size distribution of the chiral gold nanoparticles is determined by ImageJ based on TEM images of L-Au NPs (c) and D-Au NPs (d) (n=100).

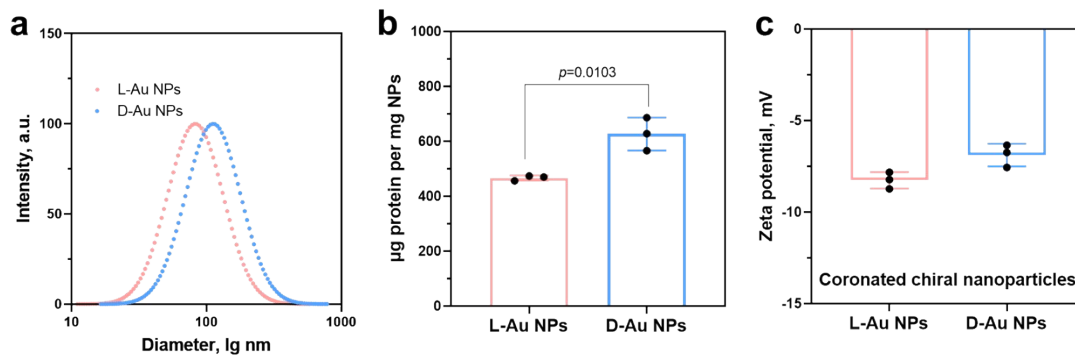


Figure S2. Hydrodynamic diameter of serum coronated chiral gold nanoparticle (a) as measured by DLS. (b) Protein amount per chiral gold nanoparticles measured by BCA assay Kit. Chiral gold nanoparticles are incubated with 10% human serum, and then the complexes of protein corona-chiral nanoparticles are obtained using centrifugation method. (c) Zeta-potential of chiral gold nanoparticle-hard corona.

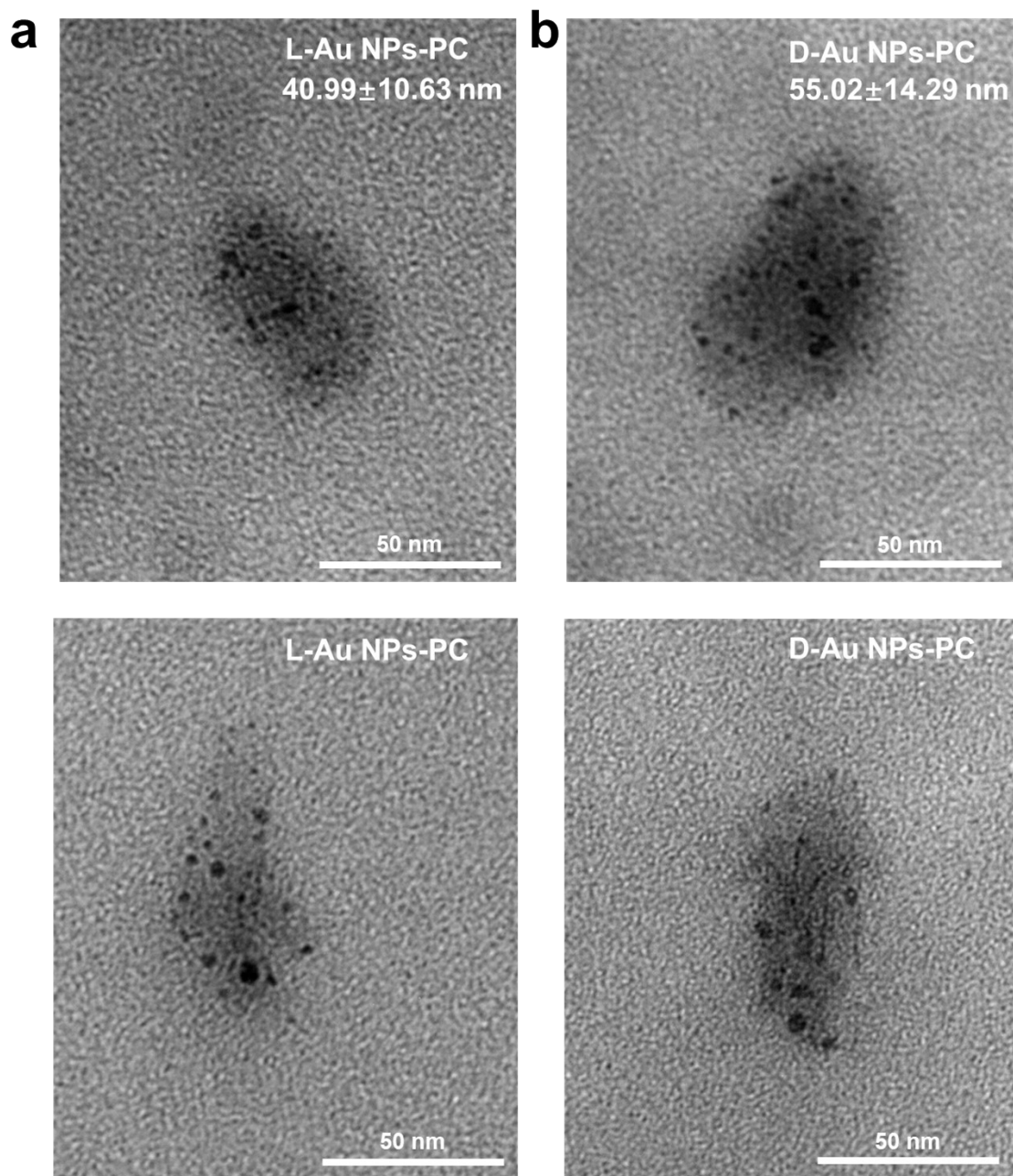


Figure S3. Representative TEM images of coronated chiral gold nanoparticles. Human serum coronated L-Au NPs (a) and D-Au NPs (b). The coronated-chiral gold nanoparticles are dropped to TEM grid with further negative staining before TEM observation. Scale bars represent 50 nm. Size distribution of the coronated chiral gold nanoparticles is determined by ImageJ based on TEM images ($n=20$).

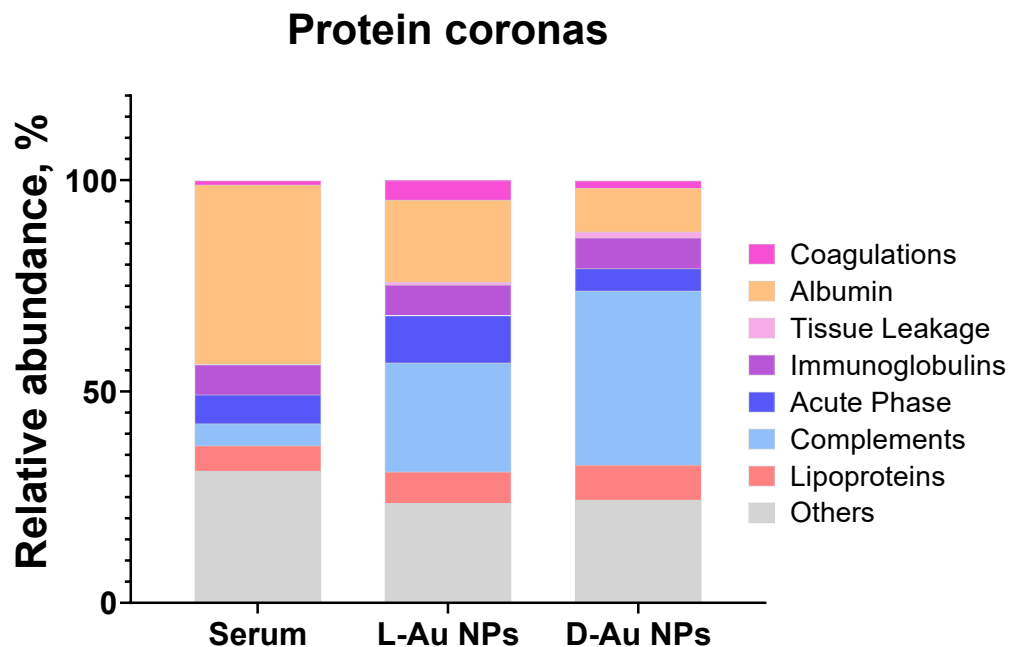


Figure S4. Protein corona composition. Identified coronal proteins of human serum and chiral gold nanoparticles are quantified by LC-MS/MS. Identified proteins were classified as coagulations, albumin, tissue leakage proteins, immunoglobulins, acute phase proteins, complements, lipoproteins, and other proteins. Protein compositions are identified by manual searching of the Human Database *via* the UniProt website. All data are shown as mean values for triplicate biological samples ($n = 3$) and standard deviations that are shown in Supplementary Tables (ESI).

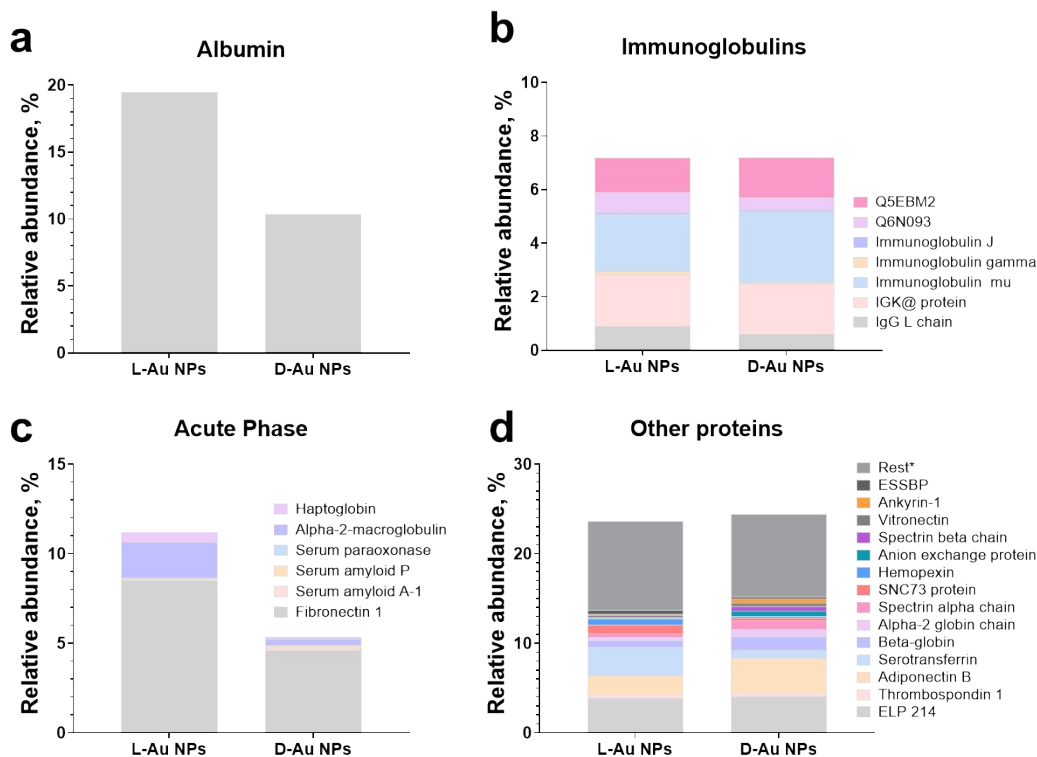


Figure S5. Classification of serum protein coronas on chiral gold nanoparticles.

Coronal components are classified based on their biological functions. Relative abundance of coronal proteins on chiral gold nanoparticles were classified into sever groups, including albumin (a), immunoglobulins (b), acute phase (c) and others (d). All data are shown as mean values for triplicate biological samples ($n = 3$) and standard deviations that are shown in Supplementary Tables (ESI).

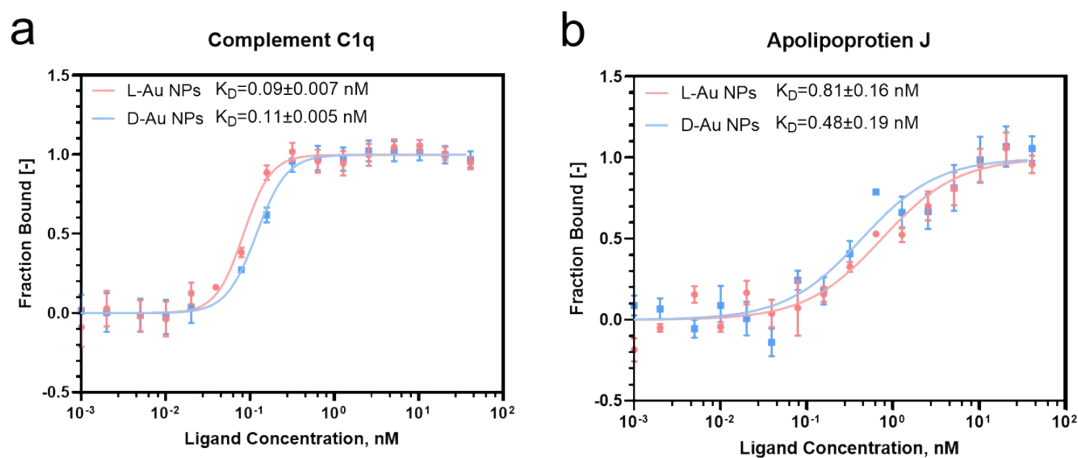


Figure S6. Thermodynamic and kinetic aspects of coronal protein adsorption. (a-d) Microscale thermophoresis analysis of interactions between chiral gold nanoparticles with complement C1q (a), and apolipoprotein J (b). Plots show the fraction of protein bound to the chiral gold nanoparticles at varied concentrations (0.001-40 nM, $n=3$). Dissociation constants (K_D) are obtained from non-linear fits for L-Au NPs (red) and D-Au NPs (blue). All data are shown as mean values and standard deviations.

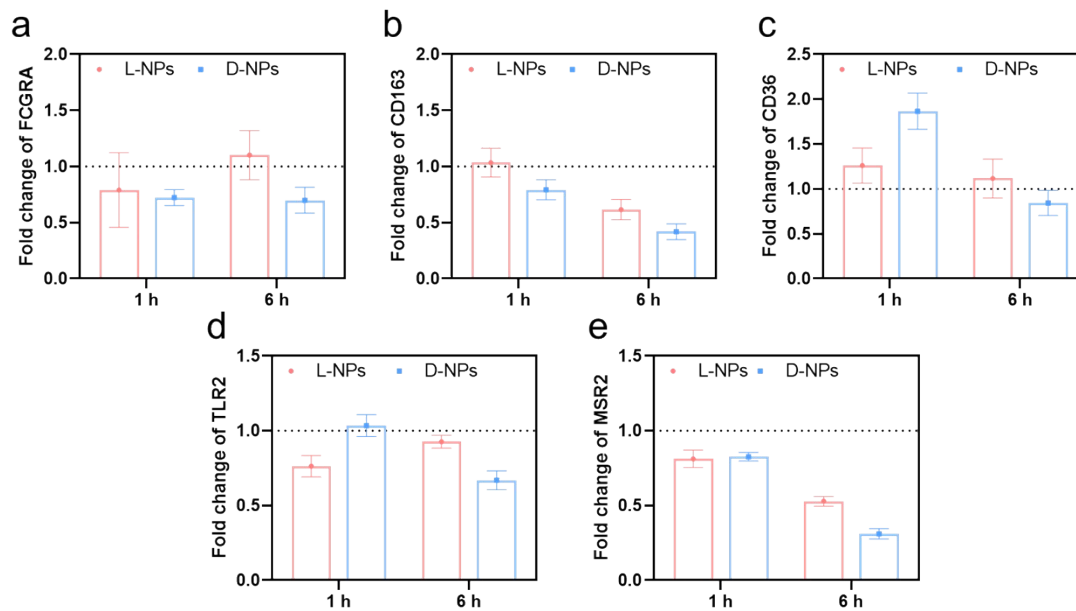


Figure S7. Expression of cell receptors upon treatment with chiral gold nanoparticles.

(a-e) Gene expression of receptors by macrophages upon treatment with L-Au NPs and D-Au NPs, including FCGRA (a), CD163 (b), CD36 (c), TLR2 (d) and MSR2 (e) determined by RT-qPCR. All data are shown as mean values and standard deviations for three biological replicates (n = 3).

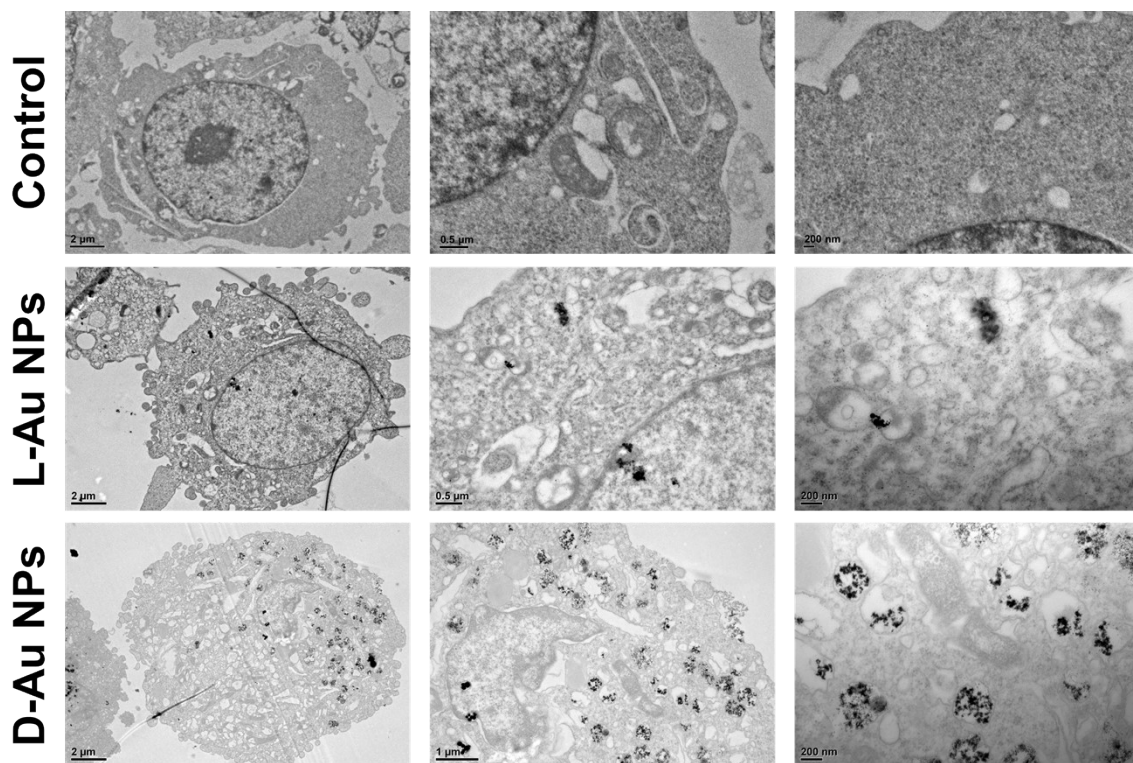


Figure S8. TEM images for macrophage uptake of chiral gold nanoparticles. THP-1 cells are treated with chiral gold nanoparticles at 20 $\mu\text{g}/\text{mL}$ for 24 h supplied with 10% human serum-containing cell culture medium and captured by TEM. Scale bars represent 2 μm , 500 nm and 200 nm, respectively.

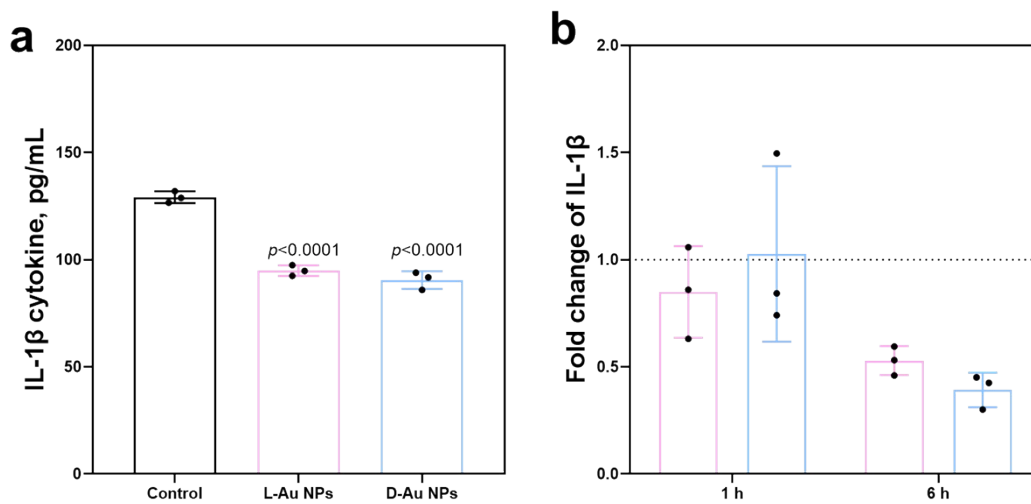


Figure S9. Secretion of pro-inflammatory cytokines by macrophages. (a, b) IL-1 β cytokine secretion (a) as determined by ELISA, and cytokine gene expression (b) as determined by RT-qPCR. Chiral NPs at 20 $\mu\text{g}/\text{mL}$ are introduced in 10% human serum supplied culture media. Data are shown as mean values and standard deviations for three biological replicates ($n = 3$).

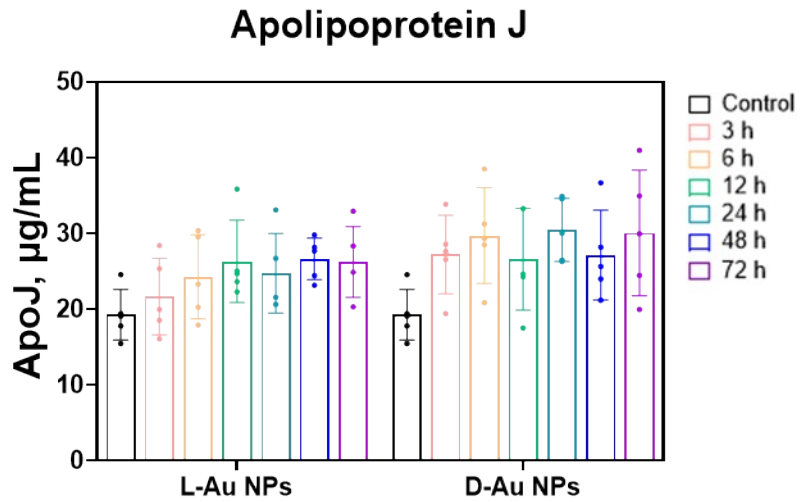


Figure S10. *Ex vivo* serum protein level of clusterin. Mice serum clusterin level is determined by ELISA Kit assay. Statistical significance is calculated by two-way ANOVA with Tukey's multiple comparisons test. All data are shown as mean values and standard deviations for five biological replicates (n = 5).

Table S1. The twenty most abundant coronal proteins.

Serum		L-Au NPs		D-Au NPs	
Albumin	42.455 ± 0.585%	Albumin	19.468 ± 2.23%	Complement C3	19.693 ± 1.466%
Serotransferrin	7.230 ± 0.220%	Complement C3	11.409 ± 3.218%	Albumin	10.375 ± 1.343%
ELP214	6.557 ± 1.252%	Fibronectin 1,	8.495 ± 1.534%	Complement C4-A	4.708 ± 0.326%
Alpha-2-macroglobulin	4.711 ± 1.234%	ELP 214	3.896 ± 1.671%	Complement factor H	4.701 ± 0.981%
Apolipoprotein A-I	4.251 ± 0.199%	Complement C4-A	3.559 ± 0.557%	Fibronectin 1	4.625 ± 1.491%
SNC73 protein (SNC73)	2.674 ± 0.138%	Serotransferrin	3.147 ± 1.487%	ELP214	4.047 ± 0.331%
IGK@ protein	2.367 ± 0.244%	Complement factor H	2.992 ± 0.484%	Adiponectin B	3.821 ± 0.345%
Complement C3	2.138 ± 0.201%	Apolipoprotein A-I	2.886 ± 0.862%	Platelet factor 4	3.548 ± 0.295%
ESSBP	1.648 ± 0.304%	Platelet factor 4	2.741 ± 0.152%	Apolipoprotein C-III	2.868 ± 0.043%
Haptoglobin	1.619 ± 0.588%	IGH μ	2.133 ± 0.251%	Complement C1qB	2.862 ± 0.215%
IGH μ	1.455 ± 0.458	Adiponectin B	2.132 ± 1.093%	IGH μ	2.649 ± 0.212%
UP Q6N093	1.295 ± 0.079%	Apolipoprotein C-III	2.009 ± 0.125%	Apolipoprotein A-I	2.47 ± 0.279%
IgG L chain	1.280 ± 0.213%	Alpha-2-macroglobulin	1.992 ± 0.611%	C4b-binding protein alpha	2.009 ± 0.234%
Hemopexin	1.099 ± 0.008%	IGK@ protein	1.924 ± 0.861%	IGK@ protein	1.89 ± 0.198%
Complement C4-A	1.007 ± 0.339%	Complement C1qB	1.8 ± 0.677%	Complement C1qA	1.746 ± 0.275%
Beta-globin	0.993 ± 0.295%	Fibrinogen beta chain	1.67 ± 0.403%	Beta-globin	1.585 ± 0.345%
Alpha-1-acid glycoprotein	0.791 ± 0.135%	Fibrinogen gamma chain	1.643 ± 0.566%	Properdin	1.514 ± 0.217%

Coagulation factor V	$0.707 \pm 0.173\%$	C4b-binding protein alpha	$1.438 \pm 0.342\%$	UP Q5EBM2	$1.503 \pm 0.244\%$
CP protein	$0.643 \pm 0.008\%$	UP Q5EBM2	$1.281 \pm 0.272\%$	Complement component 9	$1.446 \pm 0.149\%$
Apolipoprotein C-III	$0.625 \pm 0.141\%$	SNC73 protein (SNC73)	$1.03 \pm 0.347\%$	Spectrin alpha chain	$1.021 \pm 0.287\%$
Transthyretin	$0.618 \pm 0.053\%$	Complement C1qA	$0.938 \pm 0.594\%$	Clusterin	$0.985 \pm 0.084\%$

Note. The list of twenty most abundant proteins of human serum (86%), on L-Au NP (79%) and D-Au NPs (80%) are listed. Identified proteins are the average of three biological replications of each sample. All data are shown as mean values and standard deviations for triplicate biological samples (n = 3).

Table S2. Enrichment factors of the chiral gold nanoparticles.

Proteins	Enrichment factor	
	L-Au NPs	D-Au NPs
Complement C1qA	90.44 ± 57.29%	168.43 ± 26.55%
Complement C1qB	6.82 ± 2.56%	10.85 ± 0.81%
Complement C1s	9.07 ± 2.31%	12.35 ± 1.11%
Complement C3	5.52 ± 1.55%	9.51 ± 0.72%
Complement C1r	9.27 ± 0.53%	10.73 ± 0.48%
Complement C9	19.84 ± 8.19%	37.64 ± 3.88%
Complement C8B	4.96 ± 1.82%	7.99 ± 0.84%
Complement factor H1	5.02 ± 0.81%	7.89 ± 1.65%
Fibrinogen alpha	10.54 ± 1.43%	4.56 ± 2.13%
Fibrinogen beta	16.59 ± 2.38%	4.26 ± 3.27%
Fibrinogen gamma	163.99 ± 25.61%	43.38 ± 3.38%
Fibronectin 1	20.56 ± 3.71%	11.20 ± 3.61%
Apolipoprotein A-I	0.70 ± 0.45%	0.60 ± 0.07%
Apolipoprotein A-II	1.07 ± 0.08%	0.75 ± 0.07%
Apolipoprotein A-IV	2.48 ± 0.38%	2.93 ± 0.70%
Apolipoprotein B	1.23 ± 0.88%	0.88 ± 0.17%
Apolipoprotein C-I	2.49 ± 0.52%	3.67 ± 0.59%
Apolipoprotein C-III	3.31 ± 0.21%	4.72 ± 0.07%
Apolipoprotein E	17.50 ± 1.51%	25.56 ± 1.38%

Note. Enrichment factors were calculated as the abundance of a protein onto chiral gold nanoparticles compared to that in the serum. Proteins with enrichment factor beyond 10 were marked bold.

Table S3. STRING score.

Proteins	Receptors	Score	Abundance (%) on	
			L-Au NPs	D-Au NPs
Complements				
C1QA	CD163	0.859	0.94%	1.75%
C1QB	CD163	0.871	1.80%	2.86%
C1QC	CD163	0.769	2.13%	3.82%
C3	ITGAM	0.996	11.41%	19.69%
C3	CR1	0.999		
Acute phase				
FN1	CD163	0.716	8.49%	4.62%
FN1	TLR2	0.799		
FN1	ITGAM	0.959		
Lipoproteins				
APOA1	LDLR	0.969	2.89%	2.47%
APOA1	CD36	0.718		
APOE	LDLR	0.998	0.29%	0.42%
APOE	MSR1	0.758		
APOC3	LDLR	0.953	2.00%	2.87%
APOC3	TLR2	0.888		
APOA4	LDLR	0.937	0.72%	0.85%
Albumin				
ALB	TLR2	0.707	19.47%	10.37%
ALB	ITGAM	0.756		
Coagulations and other				
FGB	ITGAM	0.908	1.67%	0.43%
FGA	ITGAM	0.932	0.73%	0.31%
FGG	ITGAM	0.936	1.64%	0.43%
THBS1	CD36	0.989	0.40%	0.45%
IGH μ	FCGR2A	0.853	2.13%	2.65%

References

1. D. Baimanov, J. Wang, J. Zhang, K. Liu, Y. Cong, X. Shi, X. Zhang, Y. Li, X. Li, R. Qiao, Y. Zhao, Y. Zhou, L. Wang and C. Chen, *Nat. Commun.*, 2022, **13**, 5389.
2. C. von Mering, M. Huynen, D. Jaeggi, S. Schmidt, P. Bork and B. Snel, *Nucleic Acids Res.*, 2003, **31**, 258-261.
3. E. K. Park, H. S. Jung, H. I. Yang, M. C. Yoo, C. Kim and K. S. Kim, *Inflammation Res.*, 2007, **56**, 45-50.